X-Ray Absorption Measured in the Resonant Auger Scattering Mode

Y. Hikosaka,[1] Y. Velkov,[2] E. Shigemasa,[1] T. Kaneyasu,[1] Y. Tamenori,[3] J. Liu,[2] and F. Gel'mukhanov[2]

[1]*UVSOR Facility, Institute for Molecular Science, Okazaki 444-8585, Japan*

[2]*Department of Theoretical Chemistry, Roslagstullsbacken 15, Royal Institute of Technology, S-106 91 Stockholm, Sweden*

[3]*Japan Synchrotron Radiation Research Institute, Sayo 679-5198, Japan*

(Received 23 February 2008; published 11 August 2008)

We report both experimental and theoretical studies on x-ray absorption measured in the resonant Auger scattering mode of gas phase carbon monoxide near the O1$s \rightarrow 2\pi$ region. Both experiment and theory display a crucial difference between the x-ray absorption profiles obtained in the conventional and resonant scattering modes. Lifetime vibrational interference is the main source of the difference. It is demonstrated that such interference, which arises from a coherent excitation to overlapping intermediate levels, ruins the idea for obtaining x-ray absorption spectra in a lifetime broadening free regime.

DOI: 10.1103/PhysRevLett.101.073001 PACS numbers: 33.20.Rm, 33.80.Eh, 34.10.+x

X-ray absorption spectroscopy (XAS) is one of the most powerful and versatile techniques to investigate composition, structure and electronic structure of matter, and is used not only in physics and chemistry, but now also in a variety of scientific fields such as biology and geology. The spectral ranges near the core edges of a constituent atom of interest are particularly informative parts in XAS spectra, because these ranges display characteristic core-excited structures which are sensitive to the chemical circumstance of the atom. One of the limiting factors in XAS is the spectral resolution that is restricted by the large natural widths of core-exited states; due to this physical constraint, the details of the core-excited structures are often smeared out of XAS spectra.

It has been believed that this obstacle can be removed from XAS spectra when one monitors radiative or nonradiative decay in the resonant Raman scattering condition [1,2]. The important fingerprint of resonant x-ray Raman scattering and resonant Auger scattering (RAS) is the spectral resolution which is not influenced by a lifetime broadening of core-excited states [3,4]. This fingerprint constitutes the background of the idea of XAS beyond the lifetime broadening limit of core-excited states. Tulkki and Åberg [1] suggested that lifetime broadening free XAS can be achieved by scanning over the frequencies of the incoming photons while keeping the emission frequency "fixed at the maximum of an x-ray fluorescence line." It was demonstrated by Drube *et al.* [2] that one can alternatively use Auger decay for such measurement. Narrowing of x-ray absorption resonances was also experimentally evidenced in Refs. [5,6]. Nowadays, lifetime broadening free XAS is regarded as a new powerful tool, particularly in the studies on the electronic states of solid systems.

In this Letter, we demonstrate that XAS in the lifetime broadening free regime defines core-excited states with poor accuracy. We have performed experimental and theoretical XAS studies in the RAS mode (XASRAS) around the O1$s \rightarrow 2\pi$ resonance of carbon monoxide. It is demonstrated that the XASRAS spectra exhibit profiles different to those on the conventional XAS profile. We understand that the difference results essentially from the lifetime vibrational interference (LVI) effect [4,7] arising from a coherent excitation to some overlapping vibrational levels. Our finding counsels strong caution in precise interpretations of XAS spectra measured in the lifetime broadening free regime.

The experiment was performed on the beam line 27SU [8] of SPring-8. Light from a figure-eight undulator was monochromatized by a grazing incidence monochromator. The photon bandwidth was set to around 25 meV (HWHM). The monochromatized light was introduced into a cell to which sample gases were admitted. Emitted electrons were sampled by a hemispherical electron energy analyzer (Gammadata-Scienta SES-2002) placed at a right angle with respect to the photon beam. The degree of linear polarization of the incident light was essentially 100%, and the direction of the electric vector was parallel to the axis of the electrostatic lens of the analyzer. The kinetic energy resolution of the analyzer was set to 50 meV (HWHM). The electron transmission efficiency of this analyzer setting and the kinetic energy scale of the obtained photoelectron spectra were calibrated by measuring Ne 1 s photoelectron peaks at different photon energies.

A XAS experiment in the RAS condition was performed for gas phase carbon monoxide with photon energies ω tuned near the O1$s \rightarrow 2\pi$ resonance. The right panel of Fig. 1(a) shows a total ion yield curve around the resonance which essentially corresponds to the conventional XAS. The resonance exhibits modulations due to the vibrational levels ν_c of the O1$s \rightarrow 2\pi$ state [9,10]. According to previous studies [9,10], the RAS mediated by this resonance is strongly affected by LVI, because the lifetime broadening of 0.156 eV is comparable with the vibrational intervals around 0.17 eV. We have measured more than one-hundred RAS to the $1\pi^{-1}\ A^2\Pi$ final state, in this resonance range with small photon energy step (15 meV). The results are collected in Fig. 1(a).

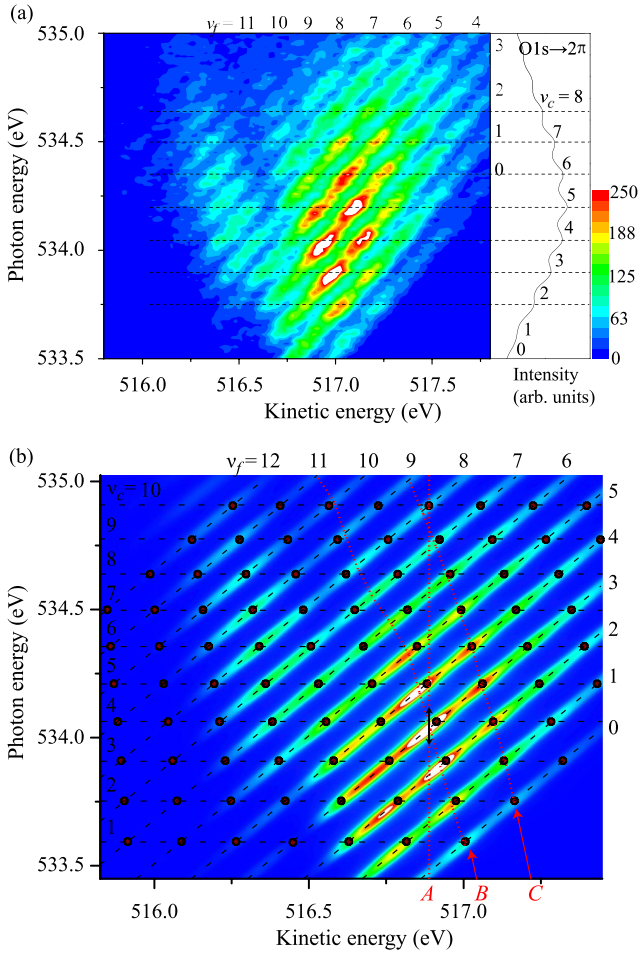

FIG. 1 (color online). (a) 2D map of the RAS yields from CO as a function of photon energy and electron kinetic energy, measured around the O1$s \rightarrow 2\pi$ resonance. The intensities on the map are plotted on a linear scale. A total ion yield curve which essentially describes the conventional XAS profile is shown in the right panel. (b) 2D map of theoretical RAS yields. The black filled circles indicate the "hilltops" resulting from the direct term $\sigma_{\mathrm{dir}}(\omega, E)$ in Eq. (4). The red dotted lines describe three paths to extract the RAS mode XAS spectra shown in Figs. 3(a)–3(c) (see text).

To explain the experiment, the RAS process was simulated with the time dependent (wave packet) code [11]. The potential energy curves for the ground, core-excited, and final ion states are assumed to be the Morse functions with parameters from the literature [10,12]. We set the natural widths (HWHM) of the core-excited and final ion states to be $\Gamma = 0.078$ eV and $\Gamma_f = 0.01$ eV, respectively, and neglected the instrumental broadening. To mimic the quasirectangular experimental photon profile, we set $\gamma = \gamma_1(\ln 2)^{1/2k} = 25$ meV (HWHM) and $k = 3$ for the spectral function of incident photons, $\Phi(\Omega, \gamma) = [k/\gamma_1\Gamma(1/2k)]\exp[-(\Omega/\gamma_1)^{2k}]$. Direct photoionization is not considered in this simulation, because the contribution is small around the resonance [10].

For an effective presentation of the experimental and theoretical RAS spectra, they were assembled as two-dimensional (2D) maps shown in Fig. 1. The horizontal axis corresponds to the electron kinetic energy E, and the vertical to the photon energy ω. The 2D maps are formed by diagonal stripes, each of which corresponds to a certain vibrational level ν_f of the final ion state. The binding energy $BE \equiv \omega - E$ is constant along the stripe and is equal to the energy $\omega_{\nu_f 0}$ of the direct transition to the final state $|0\rangle \rightarrow |\nu_f\rangle$. All stripes consist of "hills" in the shape of ellipse. It may appear at first sight that the peak positions of the hills simply reflect the ν_c progression seen in the conventional XAS spectrum; however, both experiment and theory show that the positions of the hilltops slightly deviate from the ν_c progression.

For a closer inspection of the shifts of the hilltops, the intensity distributions along the diagonal stripes ($BE = \omega_{\nu_f 0}$) were extracted from the 2D maps. In the experimental extraction, least-squares fitting with sums of Gaussian-function peaks was applied to the ν_f distribution at each photon energy. The curves thus obtained, shown in Fig. 2, correspond to the partial RAS yield curves for the formation of individual ν_f. It is clearly seen in Fig. 2 that the peak energies of each XASRAS profile do not agree with those of the ν_c progression on the conventional XAS spectrum, but instead deviate depending on the choice of final ν_f. The deviations of the resonance energies are essentially due to the LVI effect as described later. The dispersion law of the centers of gravity of the vibrationally distributed XASRAS profiles deserves a special comment. This dispersion depends on the shifts of the potential energy curves of the core-excited and final ion states relative to the equilibrium, similar to the RAS band dispersion investigated in Ref. [13].

To understand the features of the XAS profile in the RAS mode, it is instructive to adopt the time-independent representation of the RAS process. The conventional XAS profile

$$\sigma_{\mathrm{XAS}}(\omega) = \sum_{\nu_c} \frac{\langle \nu_c | 0_0 \rangle^2}{(\omega - \omega_{\nu_c 0})^2 + \Gamma^2} \qquad (1)$$

has a resonance width Γ. Here, $|0_0\rangle$ and $|\nu_c\rangle$ denote the vibrational wave functions of the ground and core-excited states, respectively, and $\omega_{\nu_c 0}$ is the resonant energy of the absorption transition $|0_0\rangle \rightarrow |\nu_c\rangle$. The spectral properties of the RAS cross section [4] $\sigma_{\mathrm{RAS}}(\omega, E) = \sum_{\nu_f} |F_{\nu_f}|^2 \Phi(\omega - E - \omega_{\nu_f 0}, \gamma)$ are given by $\Phi(\Omega, \gamma)$ and the Kramers-Heisenberg scattering amplitude

$$F_{\nu_f} = \sum_{\nu_c} F_{\nu_f \nu_c}, \quad F_{\nu_f \nu_c} = \frac{\langle \nu_f | \nu_c \rangle \langle \nu_c | 0_0 \rangle}{E - \omega_{\nu_c 0} + \omega_{\nu_f 0} + i\Gamma}, \qquad (2)$$

which is a coherent sum over the paths through different ν_c. One might expect intuitively that the RAS cross section as a function of ω should agree with the conventional XAS

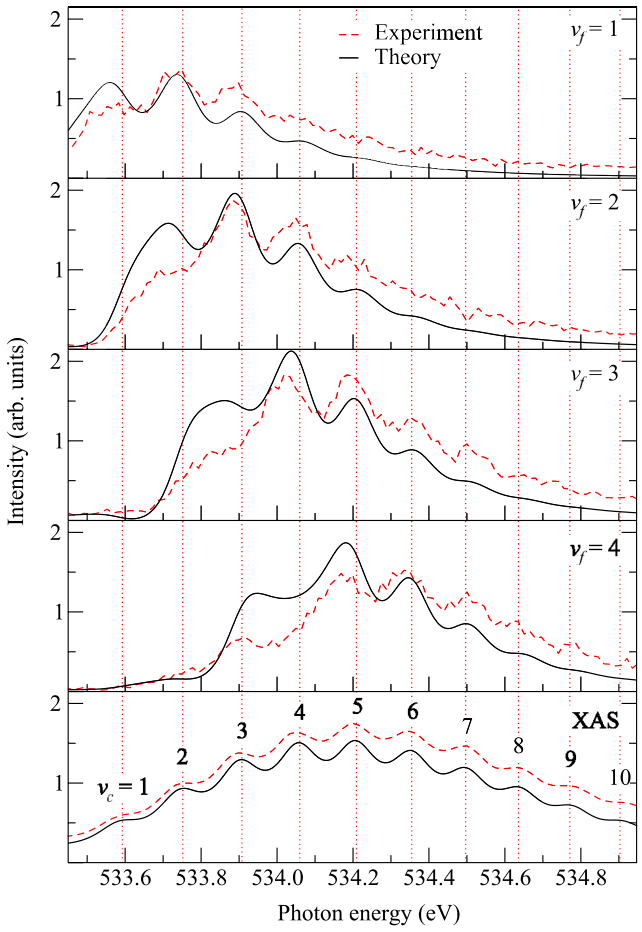

FIG. 2 (color online). Experimental (red/dashed) and theoretical (black/solid) XASRAS spectra for the formation of $\nu_f = 1$–4, extracted from the 2D maps in Fig. 1, and conventional XAS spectra.

profile, because the flux of Auger electrons is caused by x-ray absorption. However, inspection of the equations above shows that the RAS profile can deviate strongly from the conventional XAS profile due to the Franck-Condon (FC) amplitude of $\langle \nu_f | \nu_c \rangle$, the interference of the intermediate core-excited states in the terms $F^*_{\nu_f \nu_c'} F_{\nu_f \nu_c}$, and the spectral function $\Phi(\Omega, \gamma)$. It is convenient to divide the RAS cross section into direct and interference contributions:

$$\sigma_{\mathrm{RAS}}(\omega, E) = \sigma_{\mathrm{dir}}(\omega, E) + \sigma_{\mathrm{int}}(\omega, E). \tag{3}$$

According to Eq. (2), these contributions have the following form:

$$\sigma_{\mathrm{dir}}(\omega, E) = \sum_{\nu_f, \nu_c} \frac{\langle \nu_f | \nu_c \rangle^2 \langle \nu_c | 0_0 \rangle^2 \Phi(BE - \omega_{\nu_f 0}, \gamma)}{(E - \omega_{\nu_c 0} + \omega_{\nu_f 0})^2 + \Gamma^2},$$
$$\sigma_{\mathrm{int}}(\omega, E) = \sum_{\nu_f} \sum_{\nu_c' \neq \nu_c} F^*_{\nu_f \nu_c'} F_{\nu_f \nu_c} \Phi(BE - \omega_{\nu_f 0}, \gamma). \tag{4}$$

In the 2D plane of (ω, E), the direct term $\sigma_{\mathrm{dir}}(\omega, E)$ in Eq. (4) would construct hills having elliptical shapes. The peak positions of those hills have coordinates $(\omega, E) = (\omega_{\nu_c 0}, \omega_{\nu_c 0} - \omega_{\nu_f 0})$ marked by black dots in Fig. 1(b), and their locations in ω match exactly the resonances of the conventional XAS spectrum. One can see that the black dots do not coincide with the real hilltops, as the deviation was already observed in Fig. 2. The reason for the deviation is twofold: the prime reason is the contribution from the interference term $\sigma_{\mathrm{int}}(\omega, E)$ in Eq. (3). The term differs strongly from the Lorentzian shape and can have maxima at $\omega \neq \omega_{\nu_c 0}$. Thus, we understand that LVI between different ν_c causes the shifts of the hilltops. The second reason is the overlap between hills, which is dependent on the choice of ν_f. This can be judged from the fact that $\sigma_{\mathrm{dir}}(\omega, E)$ includes the additional FC amplitudes $\langle \nu_f | \nu_c \rangle^2$ as compared with Eq. (1).

The easiest way to envisage the XASRAS spectral resolution is to look at the direct term in Eq. (4). The cross sections along the major elliptical axes ($BE = \omega_{\nu_f 0} = \mathrm{const}$) passing through the peaks of the hills,

$$\sigma_{\mathrm{dir}}(\omega, E) = \Phi(0, \gamma) \sum_{\nu_c} \frac{\langle \nu_f | \nu_c \rangle^2 \langle \nu_c | 0_0 \rangle^2}{(\omega - \omega_{\nu_c 0})^2 + \Gamma^2}, \tag{5}$$

would not display better resolution than Γ, because the spectral function is just a constant factor. In agreement with this inspection, the XASRAS spectra in Fig. 2 do not show better resolution than the natural width of the core-excited state. On the other hand, the cuts of the hills along the ω axis ($E = \omega_{\nu_c 0} - \omega_{\nu_f 0} = \mathrm{const}$),

$$\sigma_{\mathrm{dir}}(\omega, E) = \frac{1}{\Gamma^2} \langle \nu_f | \nu_c \rangle^2 \langle \nu_c | 0_0 \rangle^2 \Phi(\omega - \omega_{\nu_c 0}, \gamma), \tag{6}$$

provide supernarrow resonances whose widths are equal to the spectral-function width γ. In practice, each hill on the individual diagonal stripes on the 2D maps (Fig. 1) show a narrower width along the ω axis. The idea of lifetime broadening free XAS relies on this fact.

Figure 3(a) shows XASRAS spectra of superhigh resolution extracted from the 2D maps along the ω axis. The theoretical spectrum corresponds to the cut going through the peak position of the global maximum on the 2D map at $E = E_{\mathrm{max}} = 516.89$ eV, which is indicated in Fig. 1(b) as path A, while the experimental one results from the integration of the yields in $E = 516.93$–516.97 eV. Both the experimental and theoretical spectra show sharp peaks whose widths are apparently narrower than the natural width of the core-excited state. This is because the RAS cross section $\sigma_{\mathrm{RAS}}(\omega, E_{\mathrm{max}})$ of Eq. (3) is simply proportional to the narrow spectral function $\Phi(\omega - E_{\mathrm{max}} - \omega_{\nu_f 0}, \gamma)$. However, the peak positions of the resonances, do not coincide with the vibrational levels of the core-excited state, but instead follow fully the vibrational progression (intervals around 190 meV) of the final ion state, since the spectral function has maxima at $\omega = E_{\mathrm{max}} + \omega_{\nu_f 0}$. It should be noted that this way of the extraction gives resonances coinciding with ν_c, only when

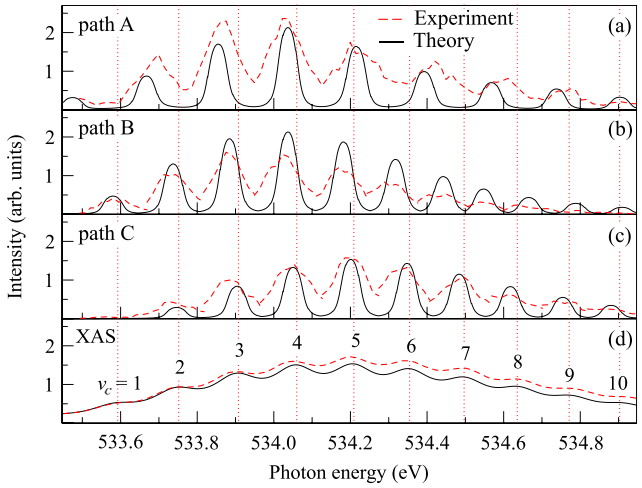

FIG. 3 (color online). (a) XASRAS spectra extracted along the ω axis in the 2D maps in Fig. 1. The theoretical spectrum (black/solid) corresponds to the cut of the theoretical 2D map at $E = 516.89$ eV [path A indicated in Fig. 1(b)], while the experimental one (red/dashed) results from the integration of the yields in $E = 516.93$–516.97 eV. (b) XASRAS spectra extracted along path B which is indicated in Fig. 1(b). (c) The same as (b) for path C. (d) Conventional theoretical and experimental XAS spectra.

the potential surfaces of core-excited and final states are fully parallel to each other [6].

Apparently, XASRAS spectroscopy of superhigh resolution is meaningful only if it gives the same positions of the resonances as the conventional XAS. In an effort to overcome the problem in the XASRAS profile copied of the ν_f progression, instead of the vertical path through the global maximum, a more sophisticated path which follows the local maxima of the hills should be adopted in extracting a XASRAS spectrum. In this way of extraction, we can obtain a narrow XASRAS resonance by scanning over ω in the vicinity of a hill while keeping E fixed at the hilltop. To get the rest of the resonances, we need to tune E to the corresponding hilltops. However, we face here the ambiguity in the choice of the path through the hilltops, though there is no real problem only if all paths give the same XASRAS profiles as the conventional XAS. To check this point we selected paths B and C shown in Fig. 1(b). One can see that both paths deviate differently from the black dots coinciding with the ν_c peaks of the conventional XAS profile and with the resonances of the direct scattering $\sigma_{\mathrm{dir}}(\omega, E)$ (4). The deviation is mainly due to the LVI, as already discussed with the help of Fig. 2 and Eq. (4). The deviation observed means that this method of XASRAS extraction provides narrow resonances coinciding with the XAS peaks only when the LVI is negligibly small.

The XASRAS spectra at superhigh resolution, resulting from the extraction following paths B and C, are presented in Figs. 3(b) and 3(c), respectively. The positions of the XASRAS resonances disagree with the XAS resonances, and the peak deviations as well as the envelopes are sensitive to the choice of path; the interference effect ruins the idea of x-ray absorption spectroscopy beyond the lifetime broadening. The lifetime broadening free regime is to be desired, essentially when the spacings between core-excited levels are smaller than Γ and the resonance maxima of the core-excited levels are hardly recognizable on conventional XAS resonances. Since the interference between the core-excited levels is strong in such cases, the resultant XASRAS profiles obtained in "the lifetime broadening free regime" is profoundly different from the conventional XAS ones.

In conclusion, we argue that the LVI effect at molecular core-excited states causes XAS profiles observed in the RAS mode to differ from the conventional XAS profiles. Although the extractions of RAS yields along the ω axis obey spectral resolution beyond the natural width of the core-excited state, the resonant energies on the XASRAS spectra deviate from the real resonance energies of the x-ray absorption. The present work demonstrates clearly that interferences arising from coherent core excitation to overlapping electronic or vibrational levels spoils the idea of obtaining XAS spectra in a lifetime broadening free regime.

We thank Professor J. H. D. Eland (PTCL) for a careful reading of the manuscript and Professor N. Kosugi (IMS) for fruitful discussion. The experiment was carried out with the approval of the JASRI (Proposals No. 2006B1500 and No. 2007A1866). This work has been supported by the Swedish Research Council (VR), the STINT foundation, National Basic Research Program of China with Grant No. 2006CB806000, and the Japan Society for Promotion of Science.

[1] J. Tulkki and T. Åberg, J. Phys. B **15**, L435 (1982).
[2] W. Drube, A. Lessmann, and G. Materlik, in *Resonant Anomalous X-Ray Scattering. Theory and Applications*, edited by G. Materlik, C. J. Sparks, and K. Fisher (North-Holland, Amsterdam, 1994), p. 473.
[3] P. Eisenberger *et al.*, Phys. Rev. Lett. **36**, 623 (1976).
[4] F. Gel'mukhanov and H. Ågren, Phys. Rep. **312**, 87 (1999).
[5] K. Hämäläinen *et al.*, Phys. Rev. Lett. **67**, 2850 (1991).
[6] A. Kivimäki *et al.*, Phys. Rev. Lett. **81**, 301 (1998).
[7] F. Gel'mukhanov *et al.*, Chem. Phys. Lett. **46**, 133 (1977).
[8] H. Ohashi *et al.*, Nucl. Instrum. Methods Phys. Res., Sect. A **467–468**, 529 (2001).
[9] M. Neeb *et al.*, J. Electron Spectrosc. Relat. Phenom. **67**, 261 (1994).
[10] T. Tanaka *et al.*, Phys. Rev. A **72**, 022507 (2005).
[11] P. Sałek, Comp. Phys. Comm. **150**, 85 (2003).
[12] K. P. Huber and G. Herzberg, *Molecular Spectra and Molecular Structure IV* (Van Nostrand Reinhold, New York, 1979).
[13] F. Gel'mukhanov and H. Ågren, Phys. Rev. A **54**, 3960 (1996).